Contents lists available at ScienceDirect

## Colloids and Surfaces A: Physicochemical and Engineering Aspects

# Yield stress and elasticity of aqueous foams from protein and surfactant solutions – The role of continuous phase viscosity and interfacial properties

M. Lexis *, N. Willenbacher

*Department of Chemical Engineering, Karlsruhe Institute of Technology, 76131 Karlsruhe, Germany*

## HIGHLIGHTS

- We discuss the influence of liquid phase viscosity on yield stress and storage modulus of aqueous foams.
- We investigate the correlation between foam rheology and interfacial rheology.
- Higher interfacial elasticity increases yield stress and storage modulus of the foams.
- Aggregation of proteins lowers interfacial but increases foam elastic modulus.

## GRAPHICAL ABSTRACT
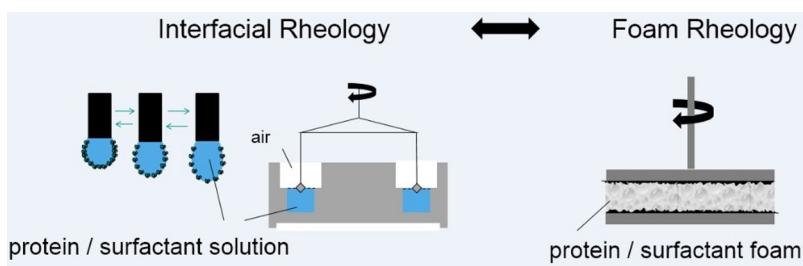
## ABSTRACT

We discuss the effect of solvent viscosity $\eta_L$ and interfacial elasticity ($E'$, $G'$) on apparent yield stress $\tau_y$ and storage modulus $G_0$ of protein and surfactant foams made from solutions of these amphiphiles in various water/glycerol mixtures. The critical volume fraction at which $\tau_y$ and $G_0$ occur is calculated from the bubble size distribution and is related to the adsorption kinetics of the corresponding amphiphile. Dependence of $\tau_y$ on $\eta_L$ is weak ($\tau_y \sim \eta_L^{0.3}$). Generally, higher interfacial moduli correspond to higher $\tau_y$ and $G_0$, but the relationship is non-trivial when protein interaction and structure formation get relevant. Increasing glycerol fraction reduces electrostatic interaction range and solvent quality for the proteins. This leads to an increase in $E'$ as well as $G_0$ for casein. For whey protein isolate (WPI) at 1% concentration, this results in an increase in $G_0$, a decrease in $E'$, and a broad transition region between linear and non-linear stress response. These findings are consistently attributed to protein aggregation finally resulting in network formation across lamellae. This network does not form at 0.1% WPI concentration and accordingly $G_0$ increases with WPI concentration. In contrast, $\tau_y$ remains constant suggesting that this network is destroyed at this stress level.

© 2014 Elsevier B.V. All rights reserved.

## 1. Introduction

Aqueous foams are dispersions of gas in a liquid. Here, we restrict ourselves to dispersions with gas volume fractions beyond the maximum packing fraction $\phi_c$ at which gas bubbles start to deviate from their spherical shape. The bubbles need to be stabilized, e.g. by amphiphilic molecules like surfactants or proteins. Foams can be found in numerous industrial applications and especially in the food sector the creation of foamed products is a rapidly growing process [1]. From a rheological point of view foams are complex systems that exhibit viscoelastic behavior and an apparent yield stress. Below a critical shear stress the jammed foam bubbles

* Corresponding author. Tel.: +49 72160842805.
*E-mail address:* meike.lexis@kit.edu (M. Lexis).

do not move past each other. In this regime foams behave as viscoelastic solids with $G' \gg G''$ and initially start flowing above this critical stress, called apparent yield stress.

Investigation of the parameters having an impact on the yield stress of foams as well as the elastic properties at low stresses has been subject to many studies [2–9]. Most of the studies were performed on surfactant foams or emulsions (as model system for foams) and some additionally on protein foams. They all agree in the point that the crucial parameters determining foam rheology are gas volume fraction, surface tension, as well as bubble size distribution. Generally, the yield stress and the storage modulus were found to be proportional to $(\sigma/r_{32})^*\phi^2$ where $\sigma$ is the surface tension, $r_{32}$ the Sauter mean radius and $\phi$ the gas volume fraction. Some authors additionally mention the continuous phase viscosity and the interfacial viscoelasticity of the adsorbed layer to be important for the stability [10] and the rheology [9,11] of foams but systematic investigation is missing in the literature.

Adsorbed protein layers at liquid/gas interfaces show viscoelastic behavior, when the surface concentration is sufficiently high due to an evolving contact network. The classical, most often used explanation is attractive interactions resulting from covalent cross-linking [12,13]. The underlying mechanisms are analogous to the gelling caused by heat or chemical denaturation [14]. However, several studies executed on protein films at the air/water interface have not been able to confirm that covalent cross-linking is the dominating source of interfacial elasticity [14–18]. Instead they propose a colloidal view of the protein layers [19,20] where the interfacial elasticity is a result of densely packed loose proteins. Cicuta et al. [19] showed that an adsorbed layer of β-lactoglobulin behaves similarly to an adsorbed layer of colloidal polystyrene particles. Elastic behavior sets in when a maximum packing fraction at the interface is exceeded and the protein molecules start to act like soft disks.

The surface dilational modulus is often referred to as the crucial surface layer property determining the foam stability. Unfortunately, the studies of interfacial viscoelasticity are mainly focused on small protein concentrations that are substantially lower than the concentrations needed to create stable foams [21–24].

In the present work, we discuss the parameters influencing the rheological foam properties yield stress $\tau_y$ and storage modulus $G_0$. In order to cover a broad variety of interfacial features we worked with different protein and surfactant systems that are known to create different interfacial layers. We suggest a phenomenological expansion of Masons equations [4,5] for $\tau_y$ and $G_0$ including the liquid viscosity $\eta_L$. Moreover, we present a way to predict the critical gas volume fraction $\phi_c$ from the bubble size distribution in the foam based on a model equation developed for the calculation of the maximum packing fraction of solid spheres with arbitrary particle size distribution. Additionally, we characterize the surface elasticity in dilation and shear and discuss the relationship between interfacial viscoelastic properties and bulk foam rheology. All measurements on the solutions and foams were carried out at equal protein or surfactant concentrations enabling a direct comparison of interfacial and macroscopic foam properties.

Since the yield stress $\tau_y$ is a key feature regarding foam rheology we also include an elaborate discussion on the determination of this quantity and the deformation and flow of the foams investigated here at stresses below and above $\tau_y$.

## 2. Experimental details

### 2.1. Solution preparation and measurements

Surfactant foams were made from a mixture of 2% (w/w) of the nonionic surfactant Triton X-100 ($C_{14}H_{22}O(C_2H_4O)_n$, $n = 9$–10,

BASF) and 0.2% (w/w) of the anionic surfactant sodium dodecyl sulfate ($C_{12}H_{25}NaO_4S$, Roth) dissolved in different mixtures of distilled water and glycerol ($\geq$99.5%, Carl Roth). For the protein foams we used 0.1% and 1% (w/w) whey protein isolate (WPI, Fonterra) as well as 3% (w/w) micellar casein that was kindly provided by the group of Hinrichs (University of Hohenheim, Germany) and used as received. For the determination of the gas volume fraction the conductivity of the solution must be sufficiently high. The natural pH of all solutions was pH $7 \pm 0.2$.

The surface tension of all solutions was measured with the pendant drop method (Krüss, DSA 100) at 21 °C. For the protein solutions the surface tension is time dependent. After 20 min measurement time a quasi-equilibrium value was reached that was used to calculate the Laplace pressure of the foam bubbles. As the protein foams were made at higher temperatures a systematic error arises in our calculations. Niño et al. [25] found that the temperature dependence of the surface tension of the protein solutions is mainly attributed to the temperature dependent surface tension of water. Including this assumption we can estimate the error to be less than 5%.

The liquid viscosities were measured with the ARES controlled strain rheometer from TA Instruments using a double wall Couette geometry (32/34 mm). All solutions showed Newtonian behavior in the range of imposed shear rates $\dot{\gamma} = 1$–250 s$^{-1}$.

Interfacial dilational viscoelastic properties were determined at 21 °C using the oscillating bubble method (Krüss, DSA 100). The oscillations are generated by a piezo pump that pulsed with a frequency of 0.1 Hz and amplitude of 0.3. As the generation of the drop was carried out manually it was not possible to keep the drop volume for each measurement exactly the same. Hence, the amplitude resulted in a surface deformation between 2% and 3%, depending on the drop volume. The viscoelastic properties were measured at a drop age of 30 min. Therefore, oscillatory deformation was applied for a time period of 100 s and 1200 pictures were analyzed to calculate $E^* = E' + iE''$.

Interfacial shear viscoelastic properties were determined at 25 °C with the stress controlled rotational rheometer DHR3 from TA Instruments using the double wall ring geometry ($D_{\text{ring}} = 70$ mm). Details about this measuring geometry can be found in [26]. After 30 min aging of the surface the viscoelastic properties were recorded at a frequency of 0.7 Hz and a deformation amplitude of 1%. For every sample solution we confirmed that the amplitude did not exceed the linear viscoelastic regime and therefore we assume that it did not affect the network formation of the proteins.

### 2.2. Foam preparation and measurements

The protein solutions were preheated to 50 °C in a water bath to obtain foams that are stable enough for reproducible rheological measurements. At this temperature adsorption kinetics is supposed to be fast enough for quick stabilization of the gas bubbles but the temperature is still low enough to exclude protein denaturation [27]. This assumption finds confirmation in experiments (results not shown) with higher whey protein concentrations (3 wt%) where we were able to produce foams between 20 and 50 °C. Independent of process temperature, all foams showed identical yield stresses and storage moduli normalized by the Laplace pressure, thus taking into account the variation in bubble size. Furthermore, the protein solutions preheated to 50 °C and subsequently cooled down to 21 °C did exhibit the same surface tension as the untreated protein solutions. This further supports the assumption that an increase in temperature up to 50 °C does not affect the protein structure. Surfactant solutions were used at room temperature (21 °C).

For foam preparation solutions were poured on a glass filter (pore size 9–16 μm) fused in a glass pipe (diameter = 60 mm, height = 53 mm). From the bottom side nitrogen was purged

*M. Lexis, N. Willenbacher / Colloids and Surfaces A: Physicochem. Eng. Aspects 459 (2014) 177–185*

179

through the pores ($\dot{V} = 60$–80 ml/min). As soon as the foam reached the column height the nitrogen flow was stopped and recording of the foam age was started.

The time dependent gas volume fraction was determined from conductivity measurements using an electrode with integrated temperature sensor (WTW, Cond 340i). The ratio of foam to solution conductivity $\kappa$ ($\kappa = \kappa_{foam}/\kappa_{solution}$) was used to calculate the gas volume fraction (Eq. (1)) [28]

$$\phi = 1 - \frac{3\kappa(1 + 11\kappa)}{1 + 25\kappa + 10\kappa^2} \tag{1}$$

As the protein foams cool down over time the temperature dependent conductivity of the protein solutions was determined in advance. In this way the $\kappa$-values referring to the foam temperature could be calculated.

The bubble size distribution was determined from images taken with an endoscopic CCD camera (Lumenera LU 160, resolution $1392 \times 1040$) that was placed inside the foam. The Sauter mean radius $r_{32}$ was extracted from image analysis with the software iPS (Visiometrics, Germany).

Foam rheological measurements were carried out with the controlled stress rotational rheometer Rheoscope 1 (Thermofisher, Germany) using a parallel plate geometry with a diameter of 60 mm. The surfaces were covered with sandpaper and the gap was set to 6 mm to minimize wall slip effects. The measurement time was 60 s in order to limit time dependent changes in foam structure. Each foaming system was measured at different foam ages and hence, different gas volume fractions $\phi$ between 80% and 94%.

The apparent yield stress was determined from steady shear measurements. The stress was continuously increased. Depending on foam composition the initial stress was between 3 and 10 Pa and the final stress between 25 and 115 Pa. On the experimental timescales employed here the apparent yield stress was independent of start and end point of the selected stress ramp as well as on the number of data points taken. Preliminary experiments with continuous and stepwise increasing stresses (up to 6 s per data point) did not lead to significant differences in the resulting yield stress value.

The moduli $G'$ and $G''$ of the foams were determined from oscillatory shear measurements with varying stress amplitude at a frequency $f = 1$ Hz. The linear viscoelastic moduli did not show frequency dependence between 0.01 and 10 Hz. Hence, the measured $G'$-value in the linear viscoelastic regime is called plateau modulus $G_0$.

## 3. Results and discussion

### 3.1. Foam and solution properties

In Table 1 the values of the liquid viscosity $\eta_L$, the Sauter mean radius $r_{32}$ and the surface tension $\sigma$ measured for the different foam systems are summarized. Note that the mean bubble radius increases with time due to degradation processes and the liquid phase viscosity of the protein foams increases due to cooling of the foams.

### 3.2. Bubble size distribution

The bubble size distribution determines the maximum packing fraction that can be reached before the spherical bubbles start to deform. This critical value increases with broadening of the size distribution. From a physical point of view, it is the transition point where a gas dispersion turns into a jammed system with a yield stress and elastic properties [5,6]. In previous studies the critical gas volume fraction was treated as a fit parameter or an estimated value
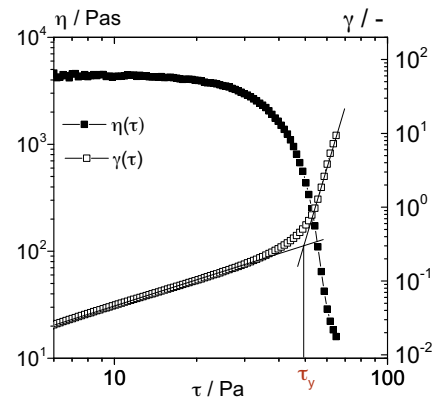


**Fig. 1.** viscosity and deformation versus shear stress for a WPI foam ($\phi = 83\%$) made from a protein solution dissolved in a water/glycerol (60/40) mixture.

between 0.63 and 0.71 for random close packing and hexagonal close packing was used, respectively.

Based on a large number of data sets Sudduth et al. [29] have proposed an empirical model to calculate the maximum packing fraction $\phi_c$ of suspensions from the size distribution of the suspended particles. Assuming a $n$-modal discrete distribution results in Eq. (2), where $\phi_{c,mono}$ is the maximum packing fraction of a monodisperse suspension ($\phi_{c,mono} = 0.63$) and $r_x$ is the $x$th moment of the particle size distribution

$$\phi_c = \phi_n - (\phi_n - \phi_{c,mono}) \exp\left(0.271 - \left(1 - \frac{r_5}{r_1}\right)\right) \tag{2}$$

with

$$\phi_n = 1 - (1 - \phi_{c,mono})^n$$

and

$$r_x = \frac{\sum_{i=1}^{n} N_i r_i^x}{\sum_{i=1}^{n} N_i r_i^{x-1}}$$

This equation is supposed to be valid for foams as well as they can be considered as highly concentrated suspensions as long as $\phi \leq \phi_c$. Hence, the critical gas volume fraction $\phi_c$ was calculated for each foam from the measured bubble size distribution.

Depending on the foam age the calculated $\phi_c$ values varied between 0.65 and 0.69 for the surfactant foams, between 0.71 and 0.75 for the 1% WPI, 0.74–0.78 for the 0.1% WPI foams and between 0.67 and 0.69 for the casein foams, i.e. in all cases the corresponding bubble size distribution broadens with time. The initial maximum packing fractions reflect very well the different adsorption behavior of the foaming agents. Time dependent surface tension measurements reveal that the surfactants used here adsorb very fast at the interface and are able to instantly stabilize the rising gas bubbles before coalescence can occur. This leads to very homogeneous bubble size distributions. Casein adsorbs slower than the SDS/Triton X100 surfactant mixture and whey protein even slower than casein. Accordingly, the width of the bubble size distribution increases in the order surfactant, casein, whey protein and this is directly reflected in the corresponding $\phi_c$ values.

### 3.3. Steady shear measurements

Steady shear measurements with increasing applied stress provide flow curves that are usually used to determine the viscosity in dependence of the shear stress or strain rate and if applicable the yield stress is deduced. For the foams used in this study the measured viscosity vs. shear stress curves usually split up into two sections as exemplary shown in Fig. 1 exemplary for a WPI foam. In

**Table 1**
Measured liquid viscosities $\eta_L$, Sauter mean radius $r_{32}$ and surface tension $\sigma$ for the different foaming systems. The given ranges are according to initial and final foam ages where the rheological measurements took place. The maximum deviations of the measured values from the average data listed above are given in the last line.

| Glycerol/% | Surfactants | | | WPI 1%   WPI 0.1% | | | Casein | | |
|---|---|---|---|---|---|---|---|---|---|
| | $\eta_L$/mPa s | $r_{32}$/μm | $\sigma$/mN/m | $\eta_L$/mPa s | $r_{32}$/μm | $\sigma$/mN/m | $\eta_L$/mPa s | $r_{32}$/μm | $\sigma$/mN/m |
| 0 | 1.2 | 72–177 | 31.9 | 0.8–1.1 | 96–212 | 49.8 | 1.3–1.8 | 124–166 | 48.4 |
| | | | | *0.9–1.0* | *242–328* | *52.9* | | | |
| 20 | 2.1 | 67–197 | 31.3 | 1.4–1.7 | 89–202 | 49.8 | 3.0–3.6 | 136–151 | 48.1 |
| | | | | *1.6–1.7* | *195–258* | *53.1* | | | |
| 30 | – | – | – | – | – | – | 3.8–4.8 | 177–186 | 47.5 |
| 40 | 4.6 | 72–164 | 30.7 | 2.9–3.8 | 96–193 | 50.3 | – | – | – |
| | | | | *3.0–3.3* | *180–204* | *53.2* | | | |
| 60 | 12.3 | 77–192 | 30.7 | 7.5–10.5 | 131–165 | 51.2 | – | – | – |
| | | | | *7.8–10.0* | *191–209* | *52.8* | | | |
| Max. deviation/% | 1.1 | 5.1 | 0.3 | 1.3 | 10.6 | 1.5   *1.5* | 2.0 | 10.4 | 0.2 |
| | | | | *1.4* | *26.0* | | | | |

the first section we find an almost constant apparent zero shear viscosity that changes over to a shear thinning region within a narrow range of shear stresses. Theoretically there may also exist a third section at higher stresses, the high shear plateau. This regime is not found in our measurements because the foam structure changes with time and applied stress. In contrast to the value for the apparent zero shear viscosity the stress where the viscosity starts to decrease drastically does not depend on the measuring parameters at constant measurement times as already found by Møller et al. [30] for other densely packed foam and emulsion systems with an apparent yield stress. This characteristic stress is defined as the apparent yield stress. Here we determine this value by plotting the deformation versus the shear stress. Two regions with different slopes can be identified as also depicted in Fig. 1. In the first region the slope is close to 1 and hence, only small deformations occur (caused by coarsening induced bubble rearrangements). In the second region the rate of deformation drastically increases indicating foam flow. The stress at which the tangents to each regime intersect is defined as the apparent yield stress $\tau_y$ here.

We found the apparent viscosity level in the first region to strongly depend on measuring parameters like initial and final stress as well as measuring time per data point (see Fig. 2b). Similar results have already been reported by Møller et al. [30] who argue that the apparent zero shear viscosity would rise up to infinity if the measurement time would do so. From creep tests (see Fig. 2a) we are able to confirm that the apparent viscosity below the yield stress ($\tau \ll \tau_y$) monotonically increases with time. At stresses close to the yield stress the viscosity stays constant for a certain time period before it drastically decreases. Stresses higher than $\tau_y$ lead to a monotonic decrease in viscosity during the period of observation. Based on the results of Cohen-Addad et al. [31] and Vincent-Bonnieu et al. [32] we propose the following explanation. Foams are thermodynamically unstable systems and change their structure over time. Liquid films between the bubbles become thinner due to drainage and eventually burst leading to coalescence of the bubbles. At stresses far below the yield stress these local relaxations induce an apparent highly viscous flow [31]. Hence, the measured apparent viscosity is a result of the displacement of the upper plate due to bubble rearrangements induced by coalescence. The coalescence rate is correlated to the number of separating lamellae, it decreases with time and hence, the apparent viscosity increases with time. The absolute value of the yield stress of a foam decreases with foam age because the average bubbles size increases and the distribution broadens with time. This is the reason why at stresses close to, but still below the yield stress ($\tau < \tau_y$) the foam starts to flow after a certain time period, for the example shown in Fig. 2a after 160 s. Stresses far beyond the yield stress ($\tau > \tau_y$) instantly induce flow. The monotonic decrease of the viscosity is caused by the degrading processes mentioned before.

The viscosities in the shear-thinning region have to be considered as apparent values because they were not measured at steady state. From Fig. 2a it can be extracted that reaching a steady state viscosity at a given shear stress if accessible at all takes far longer than the total measurement time of 60 s employed for the stress ramp in the experiments discussed here. Such long timescales are not appropriate for the characterization of foams because of the time dependent structure evolution.

Here, we restrict ourselves to the determination of $\tau_y$ which is reproducible and robust with respect to the choice of experimental parameters. It should be noted that the determination of steady shear viscosity data is prone to systematic errors not only because the foam structure changes with time and applied stress or strain. An additional error arises because the flow profile in the shear gap is not necessarily homogeneous. Shear banding phenomena have been observed in several studies [33,34] and need to be considered when measuring foam viscosity. In Fig. 3 this is illustrated for surfactant foam but similar results were also found for the protein foams investigated here. The positions of 17 bubbles were tracked over a time period of 5 s at a constant shear rate of $\gamma = 0.2 \, \text{s}^{-1}$. Obviously, the velocity does not change linearly as it is required for a correct viscosity calculation. Instead, two flow regimes with different shear rates are observed.

### 3.4. Yield stress

Even if a true viscosity is hard to define and depends on measuring parameters, the yield stress of our foaming systems does not seem to be markedly affected by that. Varying gap sizes between 3 and 8 mm, different initial and final stresses in stress ramp experiments as well as different measuring times per data point (0.2–6 s) at a constant total measurement time of 60 s did not lead to significant differences in the yield stress. In Fig. 4, the yield stress values for all created foams are shown in dependence of $\phi - \phi_c$ where $\phi_c$ has been determined from the bubble size distribution as described in Section 3.2. The experimental data are normalized by the Laplace pressure ($\sigma/r_{32}$) in order to account for the different average bubble sizes and multiplied with the empirically determined factor $(\eta_L/\eta_W)^{-0.3}$. Here, $\eta_L$ is the continuous phase viscosity and $\eta_W$ is the viscosity of water. As already reported previously [9] this leads to a collapse of all data points for each particular foaming system onto a master curve. Based on the equation proposed by Mason [4,5], the yield stress can be described by the following empirical equation:

$$\tau_y = k \cdot \left(\frac{\sigma}{r_{32}}\right) \cdot \left(\frac{\eta_L}{\eta_W}\right)^{0.3} \cdot (\phi - \phi_c)^2 \tag{3}$$

The pre-factor $k$ is the only fit parameter in this equation, all other quantities are determined independently. Comparing the
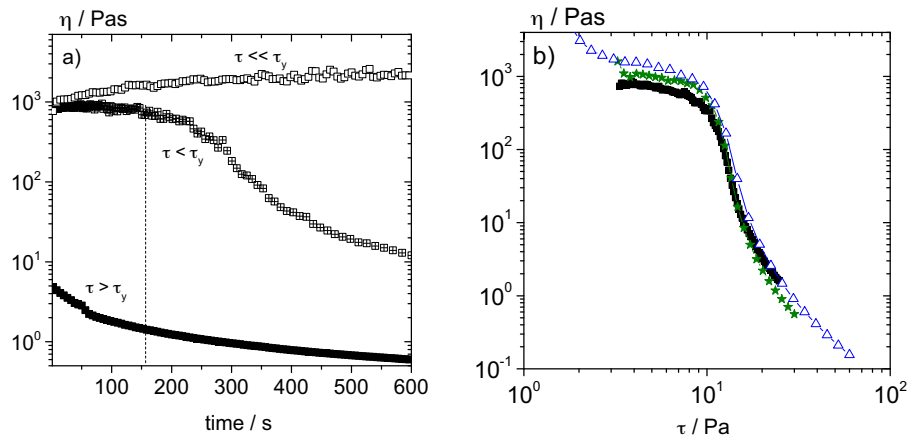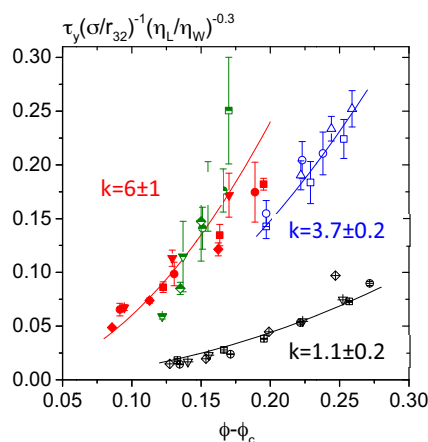
**Fig. 2.** (a) Creep tests for a foam made from the surfactant mixture dissolved in water with $\tau \ll \tau_y$ at 1 Pa (open symbols), $\tau < \tau_y$ at 8 Pa (crossed symbols) and $\tau > \tau_y$ at 20 Pa (closed symbols), (b) apparent viscosity versus shear stress for the same surfactant foam under different measurement conditions at a constant measurement time of 60 s: ■ shear stress continuously increasing from 3 to 25 Pa, ★ stepwise increase of shear stress from 3 to 30 Pa (2 s per data point), △ stepwise increase of shear stress from 1 to 60 Pa (2 s per data point).
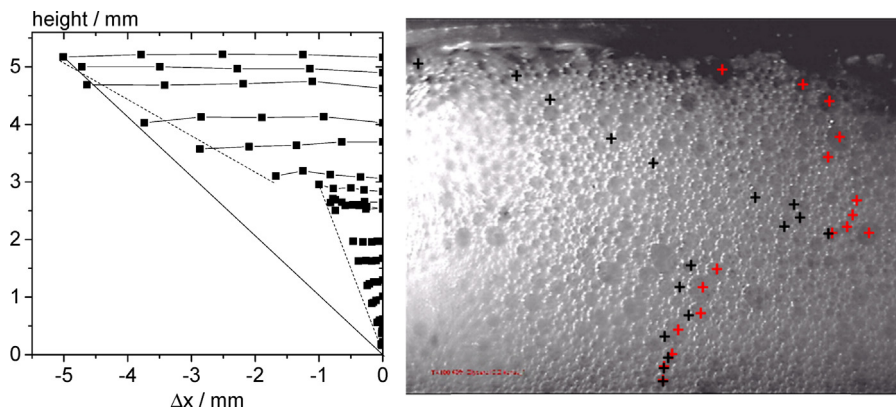


**Fig. 3.** Left side: velocity profile of a surfactant foam containing 40% glycerol at constant shear rate ($\dot{\gamma} = 0.2\,\text{s}^{-1}$). Right side: Foam image with initial bubble positions marked by red crosses and final positions reached after 5 s marked by black crosses. (For interpretation of the references to color in this figure legend, the reader is referred to the web version of this article.)

results for the different foaming systems leads to the general conclusion that the surfactant foams possess lower yield stresses than the protein foams at a given value of $\phi - \phi_c$ which in turn lie close together. The $k$-factor is 4–5 times higher for the protein foams



**Fig. 4.** Apparent yield stress $\tau_y$ normalized by Laplace pressure ($\sigma/r_{32}$) and solution viscosity ratio ($\eta_L/\eta_W$) vs. $\phi - \phi_c$ for foams made from different proteins and a surfactant mixture (closed symbols 1% WPI, semi-closed symbols 0.1% WPI, open symbols casein and crossed symbols surfactant mixture) dissolved in various water/glycerol mixtures (glycerol content ■, 0%; ●, 20%; ▼, 30%; ▲, 40%; ◆, 60%).

than for the surfactant foams. The different $k$-factors presumably arise from different interfacial layer properties as will be discussed in more detail in Section 3.6.
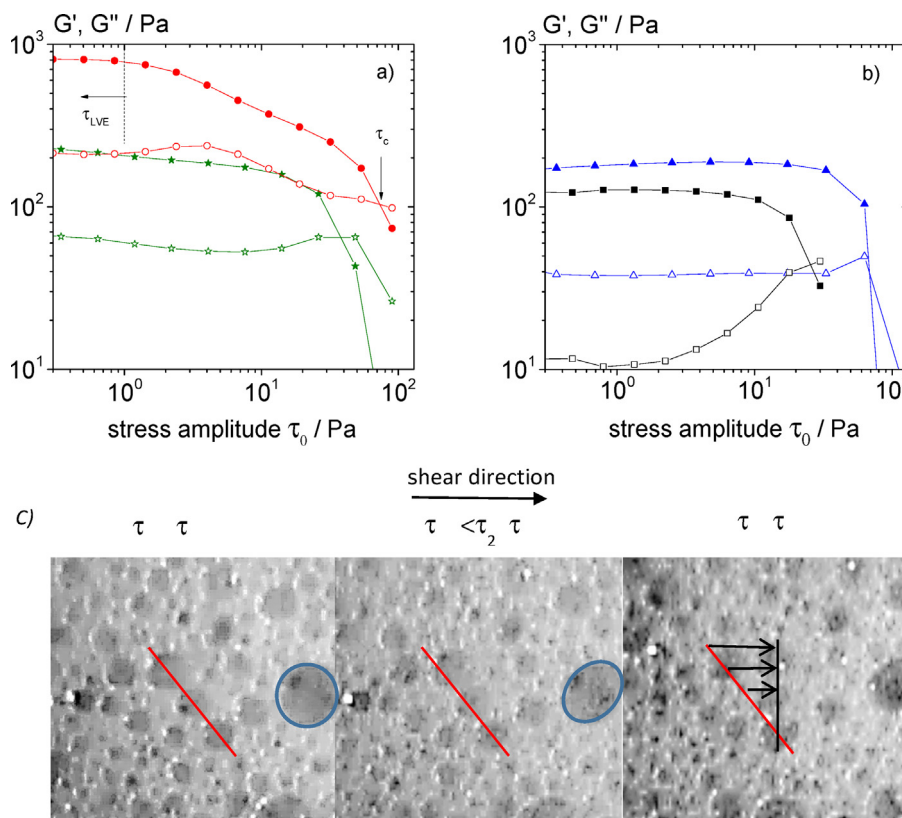
### 3.5. Oscillatory shear measurements

In Fig. 5a and b exemplary amplitude sweep curves are shown for the different foaming system but similar physical foam properties $\phi$, $\sigma/r_{32}$ and $\eta_L$. The curves keep their characteristic shape independent of glycerol content or gas volume fraction. All systems show $G' > G''$ at low stress amplitudes in the linear viscoelastic regime ($\tau_0 < \tau_{LVE}$) and $G'' > G'$ in the flow regime ($\tau_0 > \tau_c$). For the 0.1% WPI and especially for the casein system there is a sharp transition between both regimes and $\tau_c \approx \tau_{LVE}$. But for the 1% WPI and the surfactant foams a third regime can be distinguished between linear viscoelastic and flow regime. For the former the moduli decrease simultaneously and for the latter $G'$ decreases while $G''$ increases before crossing.

The 1% WPI foams exhibit high storage modulus values at very low stress amplitudes. Presumably the whey proteins build a network across the lamella that causes such high moduli. Dimitrova et al. [35] investigated the disjoining pressure in dependence of the film thickness for a 0.2 wt% β-lactoglobulin (BLG) solutions. Their results can be described by DLVO theory only for film thicknesses between 22 and 40 nm. Below these values the interaction

**Fig. 5.** Oscillatory stress amplitude sweep measurements of $G'$ (closed symbols) and $G''$ (open symbols) for (a) ● 1% WPI foam ($\phi = 0.90$, $\sigma/r_{32} = 261$ Pa, $\eta_L = 3.8$ mPa s), ★ 0.1% WPI foam ($\phi = 0.92$, $\sigma/r_{32} = 369$ Pa, $\eta_L = 3.0$ mPa s), (b) ▲ casein foam ($\phi = 0.91$, $\sigma/r_{32} = 269$ Pa, $\eta_L = 3.8$ mPa s) and ■ surfactant foam ($\phi = 0.89$, $\sigma/r_{32} = 241$ Pa, $\eta_L = 4.6$ mPa s), (c) foam images taken from video recordings during oscillatory deformation of a 1% WPI foam at different stress amplitudes. Pictures are side views of the shear gap taken at the maximum displacement during an oscillation cycle with $\tau_1 = 0.3$ Pa, $\tau_2 = 7$ Pa (bubbles deform but stay at their position), $\tau_3 = 100$ Pa (bubbles have moved).

between opposing protein layers is dominated by a steric repulsion even though the thickness of the adsorption layer, as measured for a 0.1 wt% BLG solution, is only about 3–4 nm [36]. Therefore, the authors conclude that the proteins form a network across the lamella. As BLG is the main component of the whey proteins, this might also be the case here. Intermediate stress amplitudes probably destroy this network without moving the bubbles past each other. Video recordings of the foam in the shear gap (Fig. 5c) confirm that the bubbles deform but stay at their position during the decrease of both moduli and start moving just before the moduli ross over.

The increase in $G''$ for the surfactant foams can be explained as follows. As the stress amplitude is applied some of the foam films get stretched while others are being compressed leading to regions with lower and regions with higher surfactant concentrations. In order to equilibrate this imbalance, a Marangoni flow from the compressed regions to the stretched ones is induced [37]. This is a dissipative process that becomes stronger with higher stress amplitudes and therefore should lead to an increases $G''$.

In Fig. 6 the plateau moduli normalized by Laplace pressure are plotted versus $\phi - \phi_c$. Each measurement series can be described by the equation proposed by Mason et al. (Eq. (4)) with the fit parameter a depending on the foam system

$$G_0 = a \cdot \left( \frac{\sigma}{r_{32}} \right) \cdot \phi(\phi - \phi_c) \tag{4}$$

For the surfactant foams and the 0.1% WPI foams all data points collapse onto a master curve but for the other two protein foams $G_0(\sigma/r_{32})^{-1}$ increases with increasing glycerol content. This increase is most likely not directly attributed to the increase
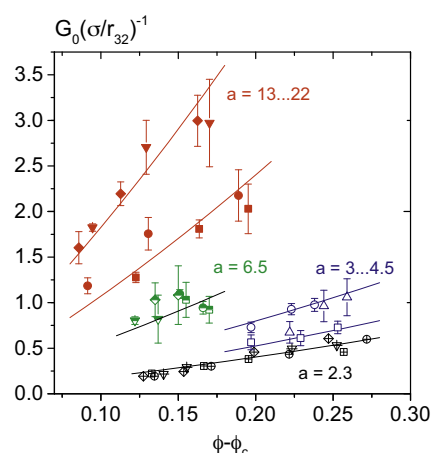


**Fig. 6.** Plateau moduli normalized by Laplace pressure vs. $\phi - \phi_c$ for foams made from 1% WPI (closed symbols), 0.1% WPI (semi-closed symbols), casein (open symbols) and surfactant mixture (crossed symbols) dissolved in various water/glycerol mixtures (glycerol content ■, 0%; ●, 20%; ▼, 30%; ▲, 40%; ♦, 60%).

in liquid viscosity since $G_0$ is an elastic modulus which is by definition not related to viscous dissipative processes. Instead this variation in the pre-factor a is due to changes in the interfacial layer properties caused by modified intermolecular interactions. The dielectric constant decreases with increasing glycerol content in the solvent mixtures [38] and hence, the range of electrostatic interactions decreases, too. This should result in a denser packing of proteins at the interface. Moreover, glycerol increases the chemical potential of the protein which decreases its solubility
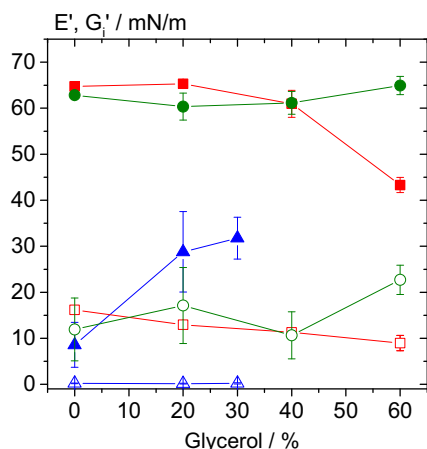
**Fig. 7.** Surface elastic moduli of WPI and casein dissolved in various water/glycerol mixtures with different glycerol content in dilation (closed symbols) and shear (open symbols) for 3% casein (triangles), 1% WPI (rectangles) and 0.1% WPI (circles). Measurements were performed after 30 min aging of the surface at a frequency of 0.1 Hz (dilation) and 0.7 Hz (shear).

[39,40]. This hypothesis is supported by the observation that dissolution of WPI is significantly slower in glycerol/water mixtures and dissolution time increases with glycerol content. Furthermore, it was not possible to dissolve the proteins in pure glycerol solution. This glycerol-induced salting-out effect occurring due to preferential hydrating of the proteins dissolved in water/glycerol mixtures was shown to apply for various proteins including β-lactoglobulin. However, it is well known that glycerol prevents denaturation of proteins and in that sense increases its stability [39,40]. Nevertheless, this change in solubility due to added glycerol may depend on the weight fraction of glycerol in the solvent, the type of protein as well as on pH and ionic strength of the solution. Various studies report an increased solubility of protein due to added glycerol, e.g. for Bovine Pancreatic Trypsin Inhibitor or T7 RNAP [49,50] but this seems not to apply for the WPI solutions investigated here. Hence, we assume that at a critical glycerol content protein aggregates should be formed and their number should increase with increasing glycerol content. Especially in the case of foams made from 1% WPI solutions these aggregates could promote the network formation across the lamellae and therefore increase foam elasticity. Foams made from 0.1% WPI solutions do not show this dramatic increase in elasticity with increasing glycerol content presumably because the solubility limit has not been reached yet and protein aggregation does not occur.

### 3.6. Interfacial rheology

The surfactants investigated here build mobile interfacial layers that do not show elastic behavior at the concentration used. The interfacial storage moduli in dilation ($E'$) and shear ($G_i'$) for the WPI and casein solutions are shown in Fig. 7. Interfacial loss moduli of all solutions were low compared to the storage moduli and are therefore not shown. For the casein solutions the elastic modulus in dilation $E'$ increases with glycerol content. Dilational deformation is sensitive to the intrinsic deformation of the molecules [41]. The decreasing range of electrostatic repulsion should result in a more compact conformation and a denser packing of proteins at the interface, thus resulting in a higher elasticity. Moreover, using glycerol for stabilizing the native structure of proteins is well known in the field of biochemistry. Gekko et al. [39,40] investigated the mechanisms behind this phenomenon and came to the following conclusion. The chemical potential of glycerol increases by contact with the protein. Since this is thermodynamically unfavorable the

system is supposed to reduce the protein–solvent interface. As a result the proteins preferably keep the compact, folded state. The most surface active component of the complex casein micelle and therefore presumably the main part of the adsorption layer is β-casein [42]. The latter is a flexible protein and the glycerol induced structure change could possibly result in a lower deformability which in turn could lead to the higher elastic dilational moduli. The shear elastic modulus $G_i'$ is very low and does not change with addition of glycerol. Cicuta et al. [43] investigated β-casein surface layers in shear and did not find elastic behavior as well. They propose that the surface mobility arises due to the loop-tail formation of these flexible molecules at the interface, i.e. at high surface concentrations the hydrophilic tails are extended into the solution [44]. When a deformation is applied this conformation possibly enables the proteins to move over or under each other in order to relax stress.

The results for 1% WPI show a different trend. The dilational modulus decreases when a glycerol content of 40% is exceeded and in shear we observe a weak monotonic decay with increasing glycerol content. Rullier et al. [45,46] investigated the structure of native and aggregated BLG with respect to the stability of foams made from these proteins. They found the aggregates to be less surface active than native proteins. However, the foam stability could be increased by adding aggregates to the native proteins. Davis and Foegeding [47] investigated the dilational elasticity of native WPI mixed with different amounts of polymerized WPI. Adding up to 50% aggregated proteins increased the dilational elasticity whereas higher amounts led to a sharp decrease in $E'$. Transferring these results to our experiments it is likely that the addition of glycerol to 1% WPI solutions leads to partial aggregation of the proteins as already suggested in Section 3.5. This in turn results in less surface activity and elasticity. The elasticity of the 0.1% WPI solutions is practically independent of glycerol content indicating that glycerol does not markedly affect the protein structure and that no significant aggregation occurs at this concentration. The surface shear experiments of the 0.1% WPI solutions show strong variations for unknown reasons and within experimental error no trend can be observed regarding the dependence on glycerol content.

### 3.7. Correlation of foam and interfacial properties

The correlation between interfacial elasticity and foam properties has been addressed in many studies. In most cases high foam stability and yield stress correspond to high interfacial elasticity [11,48].

Among the systems investigated here, the 0.1% and 1% WPI solutions show similar and highest interfacial elastic moduli and the corresponding foams exhibit the highest normalized yield stresses (see Fig. 4). Casein solutions possess lower interfacial dilational and almost no interfacial shear elasticity corresponding to lower foam yield stress. The surfactant solutions, that do not show any measurable interfacial elasticity, exhibit the lowest foam yield stresses.

According to Fig. 4 the effect of glycerol on foam yield stress is mainly due to the corresponding change in solution viscosity and captured by the scaling factor $(\eta_L/\eta_w)^{0.3}$. In contrast a complex behavior of glycerol on the surface elasticity of the protein solution is found. The decrease in E' at high glycerol content which is attributed to the formation of aggregates resulting in a network formation across the lamellae does not show up in the reduced yield stress. Presumably this network already breaks at $\tau < \tau_y$ and therefore does not contribute to the yield stress.

The relationship between protein interfacial elasticity and bulk foam elasticity is more complex. Comparing the different foaming agents investigated here we generally found highest foam elasticity for the corresponding solutions with highest interfacial elasticity. For the 0.1% WPI and the casein samples there is a direct

correlation between surface elasticity of the solution and the interfacial and bulk elasticity of the corresponding foam. Both, rheological properties of 0.1% WPI solutions and corresponding foams do not vary with glycerol content. But casein foams and solutions both become more elastic upon addition of 20% glycerol. Note, for the solution this behavior is observable only in dilation as casein solutions exhibit only very weak surface shear elasticity. In contrast, for 1% WPI solutions, the effect of glycerol on the interfacial elasticity differs from its effect on the bulk rheological properties of the foams. Adding glycerol leads to a decrease in interfacial elasticity, especially if the glycerol content of the solvent exceeds 40% whereas at the same time the foam elastic modulus drastically increases. This phenomenon is presumably due to protein aggregation. Aggregates are less surface active and decrease interfacial elasticity but probably enhance network formation across the foam lamellae and therefore increase foam elasticity.

## 4. Conclusion

We have investigated the effect of solution viscosity and surface elasticity on the apparent yield stress and bulk elasticity of foams made from protein and surfactant solutions. Whey protein solutions with different concentration, micellar casein and mixture of a non-ionic and an ionic surfactant have been employed for this study. The surface active ingredients have been used in various water/glycerol mixtures in order to study the effect of solvent viscosity on foam rheology.

Based on the equations proposed by Mason we can describe the effect of gas volume fraction and Laplace pressure on $\tau_y$ and $G_0$ (Eqs. (3) and (4)). Here we calculate the critical volume fraction $\phi_c$ from the bubble size distribution of the foams. This distribution is determined from the analysis of foam images taken with an endoscopic CCD camera. The $\phi_c$ values found for the different foaming systems are discussed in terms of foam formation and gas bubble stabilization properties of the employed proteins and surfactants. Distinct features of the transition from the linear viscoelastic region ($G' \gg G''$) to the non-linear deformation regime ($G'' > G'$) are observed for the different foam systems and can be attributed to structural features of the foam lamellae.

As expected the storage modulus $G_0$ is independent of the solution viscosity for the foams made from surfactant, casein and 0.1% WPI solutions. The increase of $G_0$ with increasing glycerol content found for the foams made from 1% WPI solutions is attributed to the formation of protein aggregates finally inducing the formation of a network structure across the lamellae.

The apparent yield stress $\tau_y$ is found to be the critical stress at which the gas bubbles start to slide past each other. This quantity directly depends on solution viscosity and this relationship is captured by an empirical factor $\left(\frac{\eta_L}{\eta_W}\right)^{0.3}$ valid for all investigated foams irrespective of gas volume fraction and type of foaming agent.

In general, protein-stabilized foams exhibit higher reduced $\tau_y$ and $G_0$ values at given ($\phi - \phi_c$) than surfactant foams. We attribute this to the surface elasticity of the corresponding solutions which is highest for both WPI solutions, significantly lower for the casein solutions and negligibly small for the surfactant solutions.

For casein a weak increase of reduced $G_0$ with increasing glycerol content is observed for the foams which corresponds to an increase in surface elasticity of the respective solutions. We attribute this to a more compact conformation of the casein molecules resulting from a decrease of solvent quality with increasing glycerol content. The 0.1% WPI system exhibits a higher foam elastic modulus $G_0$ than the casein or surfactant systems and this directly correlates to the high surface elasticity of the solution, both in shear and dilation. The scenario is more complex for the 1% WPI system. In this case the added glycerol is supposed to induce protein

aggregation. This results in a decrease of the dilation modulus $E'$ at glycerol contents beyond 20% but at the same time $G_0$ increases and we assume this is due to the formation of a network bridging the opposing protein layers across the lamellae. This network formation obviously does not affect the reduced yield stress $\tau_y$ which does not reveal a specific variation with glycerol content for the foams made from different protein solutions. Therefore we conclude that the protein network is destroyed at stresses $\tau < \tau_y$.

## References

[1] G.M. Campbell, E. Mougeot, Creation and characterisation of aerated food products, Trends Food Sci. Technol. 10 (1999) 283–296.
[2] H.M. Princen, Rheology of foams and highly concentrated emulsions, J. Colloid Interface Sci. 112 (1986) 427–437.
[3] H.M. Princen, A.D. Kiss, Rheology of foams and highly concentrated emulsions, J. Colloid Interface Sci. 128 (1989) 176–187.
[4] T.G. Mason, J. Bibette, D.A. Weitz, Elasticity of compressed emulsions, Phys. Rev. Lett. 75 (1995) 2051–2054.
[5] T.G. Mason, J. Bibette, D.A. Weitz, Yielding and flow of monodisperse emulsions, J. Colloid Interface Sci. 179 (1996) 439–448.
[6] A. Saint-Jalmes, D.J. Durian, Vanishing elasticity for wet foams: equivalence with emulsion and role of polydispersity, J. Rheol. 43 (1999) 1411–1422.
[7] S. Marze, A. Saint-Jalmes, D. Langevin, Protein and surfactant foams: linear rheology and dilatancy effect, Colloids Surf. A 263 (2005) 121–128.
[8] S. Marze, R.M. Guillermic, A. Saint-Jalmes, Oscillatory rheology of aqueous foams: surfactant, liquid fraction, experimental protocol and aging effects, Soft Matter 5 (2009) 1937.
[9] M. Lexis, N. Willenbacher, Einfluss der Flüssigkeitsviskosität auf das rheologische Verhalten von Schäumen, Chem. Ing. Tech. 85 (2013) 1317–1323.
[10] P. Wierenga, H. Gruppen, New views on foams from protein solutions, Curr. Opin. Colloid Interface Sci. 15 (2010) 365–373.
[11] J. Davis, E. Foegeding, F. Hansen, Electrostatic effects on the yield stress of whey protein isolate foams, Colloids Surf. B 34 (2004) 13–23.
[12] G.B. Bantchev, D.K. Schwartz, Surface shear rheology of β-casein layers at the air/solution interface: formation of a two-dimensional physical gel, Langmuir 19 (2003) 2673–2682.
[13] A. Williams, A. Prins, Comparison of the dilational behaviour of adsorbed milk proteins at the air–water and oil–water interfaces, Colloids Surf. A 114 (1996) 267–275.
[14] P.A. Wierenga, H. Kosters, M.R. Egmond, A.G. Voragen, H.H. de Jongh, Importance of physical vs. chemical interactions in surface shear rheology, Adv. Colloid Interface Sci. 119 (2006) 131–139.
[15] S. Roth, B.S. Murray, E. Dickinson, Interfacial shear rheology of aged and heat-treated β-lactoglobulin films: displacement by nonionic surfactant, J. Agric. Food Chem. 48 (2000) 1491–1497.
[16] A.W. Perriman, M.J. Henderson, S.A. Holt, J.W. White, Effect of the air–water interface on the stability of β-lactoglobulin, J. Phys. Chem. B 111 (2007) 13527–13537.
[17] J.T. Petkov, T.D. Gurkov, B.E. Campbell, R.P. Borwankar, Dilatational and shear elasticity of gel-like protein layers on air/water interface, Langmuir 16 (2000) 3703–3711.
[18] P. Cicuta, E.M. Terentjev, Viscoelasticity of a protein monolayer from anisotropic surface pressure measurements, Eur. Phys. J. E 16 (2005) 147–158.
[19] P. Cicuta, E. Stancik, G. Fuller, Shearing or compressing a soft glass in 2D: time-concentration superposition, Phys. Rev. Lett. 90 (2003).
[20] E. Santini, J. Krägel, F. Ravera, L. Liggieri, R. Miller, Study of the monolayer structure and wettability properties of silica nanoparticles and CTAB using the Langmuir trough technique, Colloids Surf. A 382 (2011) 186–191.
[21] R. Miller, J.K. Ferri, A. Javadi, J. Krägel, N. Mucic, R. Wüstneck, Rheology of interfacial layers, Colloid. Polym. Sci. 288 (2010) 937–950.
[22] K. Engelhardt, M. Lexis, G. Gochev, C. Konnerth, R. Miller, N. Willenbacher, W. Peukert, B. Braunschweig, pH effects on the molecular structure of β-lactoglobulin modified air–water interfaces and its impact on foam rheology, Langmuir 29 (2013) 11646–11655.
[23] J. Krägel, S. Derkatch, R. Miller, Interfacial shear rheology of protein–surfactant layers, Adv. Colloid Interface Sci. 144 (2008) 38–53.

*M. Lexis, N. Willenbacher / Colloids and Surfaces A: Physicochem. Eng. Aspects 459 (2014) 177–185*

185

[24] R. Wüstneck, J. Krägel, R. Miller, V.B. Fainerman, P.J. Wilde, D.K. Sarker, D.C. Clark, Dynamic surface tension and adsorption properties of β-casein and β-lactoglobulin, Food Hydrocoll. 10 (1996) 395–405.

[25] M. Rosario Rodríguez Niño, C.C. Sánchez, M.C. Fernández, J.M. Patino, Rodríguez, Protein and lipid films at equilibrium at air–water interface, J. Am. Oil Chem. Soc. 78 (2001) 873–879.

[26] S. Vandebril, A. Franck, G.G. Fuller, P. Moldenaers, J. Vermant, A double wall-ring geometry for interfacial shear rheometry, Rheol. Acta 49 (2010) 131–144.

[27] J. de Wit, Thermal behaviour of bovine β-lactoglobulin at temperatures up to 150 °C: a review, Trends Food Sci. Technol. 20 (2009) 27–34.

[28] K. Feitosa, S. Marze, A. Saint-Jalmes, D.J. Durian, Electrical conductivity of dispersions: from dry foams to dilute suspensions, J. Phys.: Condens. Matter 17 (2005) 6301–6305.

[29] R.D. Sudduth, A new method to predict the maximum packing fraction and the viscosity of solutions with a size distribution of suspended particles. II, J. Appl. Polym. Sci. 48 (1993) 37–55.

[30] P.C.F. Møller, A. Fall, D. Bonn, Origin of apparent viscosity in yield stress fluids below yielding, Europhys. Lett. 87 (2009) 38004.

[31] S. Cohen-Addad, R. Höhler, Y. Khidas, Origin of the slow linear viscoelastic response of aqueous foams, Phys. Rev. Lett. 93 (2004).

[32] S. Vincent-Bonnieu, R. Höhler, S. Cohen-Addad, Slow viscoelastic relaxation and aging in aqueous foam, Europhys. Lett. 74 (2006) 533–539.

[33] P. Coussot, J. Raynaud, F. Bertrand, P. Moucheront, J. Guilbaud, H. Huynh, S. Jarny, D. Lesueur, Coexistence of liquid and solid phases in flowing soft-glassy materials, Phys. Rev. Lett. 88 (2002).

[34] G. Ovarlez, S. Rodts, X. Chateau, P. Coussot, Phenomenology and physical origin of shear localization and shear banding in complex fluids, Rheol. Acta 48 (2009) 831–844.

[35] T.D. Dimitrova, F. Leal-Calderon, T.D. Gurkov, B. Campbell, Disjoining pressure vs thickness isotherms of thin emulsion films stabilized by proteins, Langmuir 17 (2001) 8069–8077.

[36] P.J. Atkinson, E. Dickinson, D.S. Horne, R.M. Richardson, Neutron reflectivity of adsorbed β-casein and β-lactoglobulin at the air/water interface, J. Chem. Soc. Faraday Trans. 91 (1995) 2847–2854.

[37] D.M.A. Buzza, C.-Y.D. Lu, M.E. Cates, Linear shear rheology of incompressible foams, J. Phys. II France 5 (1995) 37–52.

[38] L. Bergmann, C. Schaefer (Eds.), Lehrbuch der Experimentalphysik: Bd. 2 Elektromagnetismus, 8th ed., de Gruyter, Berlin, New York, 1999.

[39] K. Gekko, S.N. Timasheff, Mechanism of protein stabilization by glycerol: preferential hydration in glycerol–water mixtures, Biochemistry 20 (1981) 4667–4676.

[40] K. Gekko, S.N. Timasheff, Thermodynamic and kinetic examination of protein stabilization by glycerol, Biochemistry 20 (1981) 4677–4686.

[41] J. Maldonado-Valderrama, J.M. Rodríguez Patino, Interfacial rheology of protein–surfactant mixtures, Curr. Opin. Colloid Interface Sci. 15 (2010) 271–282.

[42] A. Saint-Jalmes, M.-L. Peugeot, H. Ferraz, D. Langevin, Differences between protein and surfactant foams: microscopic properties, stability and coarsening, Colloids Surf. A 263 (2005) 219–225.

[43] P. Cicuta, Compression and shear surface rheology in spread layers of β-casein and β-lactoglobulin, J. Colloid Interface Sci. 308 (2007) 93–99.

[44] P. Cicuta, I. Hopkinson, Studies of a weak polyampholyte at the air–buffer interface: the effect of varying pH and ionic strength, J. Chem. Phys. 114 (2001) 8659.

[45] B. Rullier, B. Novales, M.A. Axelos, Effect of protein aggregates on foaming properties of β-lactoglobulin, Colloids Surf. A 330 (2008) 96–102.

[46] B. Rullier, M.A. Axelos, D. Langevin, B. Novales, β-Lactoglobulin aggregates in foam films: correlation between foam films and foaming properties, J. Colloid Interface Sci. 336 (2009) 750–755.

[47] J. Davis, E. Foegeding, Foaming and interfacial properties of polymerized whey protein isolate, J. Food Sci. 69 (2004).

[48] P.A. Wierenga, L. van Norél, E.S. Basheva, Reconsidering the importance of interfacial properties in foam stability, Colloids Surf. A 344 (2009) 72–78.

[49] M. Farnum, C. Zukoski, Effect of glycerol on the interactions and solubility of bovine pancreatic trypsin inhibitor, Biophys. J. 76 (1999) 2716–2726.

[50] R. Sousa, Use of glycerol, polyols and other protein structure stabilizing agents in protein crystallization, Acta Crystallogr. D 51 (1995) 271–277.